

GPS constraints on the 2011–2012 Oaxaca slow slip event that preceded the 2012 March 20 Ometepec earthquake, southern Mexico

Shannon E. Graham,¹ Charles DeMets,¹ Enrique Cabral-Cano,² Vladimir Kostoglodov,² Andrea Walpersdorf,³ Nathalie Cotte,³ Michael Brudzinski,⁴ Robert McCaffrey⁵ and Luis Salazar-Tlaczani²

¹Department of Geoscience, University of Wisconsin-Madison, Madison, WI 53706, USA. E-mail: segraham@wisc.edu

²Instituto de Geofísica, Universidad Nacional Autónoma de México, Mexico City, Mexico

³Institut des Sciences de la Terre, Université de Grenoble 1, CNRS UMR 5265, F-38041 Grenoble, France

⁴Department of Geology, Miami University of Ohio, Oxford, OH 45056, USA

⁵Department of Geology, Portland State University, Portland, OR 97201, USA

Accepted 2014 January 16. Received 2014 January 16; in original form 2013 July 20

SUMMARY

We model measurements from 19 continuous GPS stations to determine the location and magnitude of a slow slip event (SSE) below southern Mexico that began in late 2011 and remained active up to the 2012 March 20 $M_w = 7.4$ Ometepec earthquake. Modelling of the space–time evolution of the SSE indicates that it initiated in 2011 November, migrated westward ~ 2.6 km per day along the subduction interface, and reached the eventual earthquake source region ~ 1 month before the 2012 March 20 earthquake occurred, in the waning stage of the SSE. The maximum slip for the SSE, ~ 100 mm, occurred ~ 100 km east of the earthquake rupture zone, in contrast to slip of 10–20 mm proximal to the Ometepec rupture zone. The SSE was focused downdip from the seismogenic zone everywhere along its ~ 300 -km-wide slip region and had a cumulative moment release of 3.0×10^{19} N•m ($M_w = 6.9$), similar to SSEs in 2004 and 2006 along this same area of the subduction interface. We calculate Coulomb stress changes as a result of slip during the SSE and find small but positive stress changes for the source region of the Ometepec earthquake. Our results are consistent with the hypothesis that the SSE triggered the Ometepec earthquake, although they are insufficient to demonstrate causality.

Key words: Space geodetic surveys; Seismic cycle; Transient deformation; Subduction zone processes.

1 INTRODUCTION

Slow slip events (SSEs), comprised of transient, aseismic fault slip that lasts for weeks to months, have been documented on many of the world's subduction zones (e.g. Schwartz & Rokosky 2007) since their discovery more than a decade ago (Dragert *et al.* 2001; Lowry *et al.* 2001). In southern Mexico, continuous GPS (cGPS) stations have recorded more than 10 SSEs since the late 1990s, all of which originated along the Guerrero or Oaxaca segments of the Mexico Subduction Zone (MSZ). The most recent of these, the subject of this study, began in late 2011 and was ongoing in 2012 March, when the $M_w = 7.4$ Ometepec thrust earthquake ruptured the seismogenic zone of the MSZ in the region of the SSE (UNAM Seismology Group 2013). As the first recorded SSE to precede a large ($M > 7$) thrust earthquake on the MSZ, it offers a unique opportunity to study possible connections between SSE and earthquakes along the MSZ, an important topic given the vulnerability of populated areas of Mexico to large MSZ earthquakes.

The principal goals of this paper are to document the GPS evidence for the 2011–2012 SSE and model its evolution in space and time with respect to both the $M_w = 7.4$, 2012 March 20 Ometepec earthquake and previously modelled SSEs in this region (Correa-Mora *et al.* 2009). This is the first in a series of papers derived from two studies of the Ometepec earthquake and the SSEs in the years preceding the earthquake (Graham 2013; Sit 2013).

2 SEISMIC HAZARD AND SLOW SLIP HISTORY OF SOUTHERN MEXICO

The subduction of the Cocos and Rivera plates along the MSZ (Fig. 1) constitutes Mexico's primary seismic hazard. During the 20th century, ~ 60 M_7+ earthquakes ruptured the MSZ (Singh *et al.* 1981; Anderson *et al.* 1989). The most destructive of these, the 1985 $M = 8.1$ Michoacan earthquake, caused more than 10 000 deaths and 3 billion dollars of damage in heavily populated Mexico City.

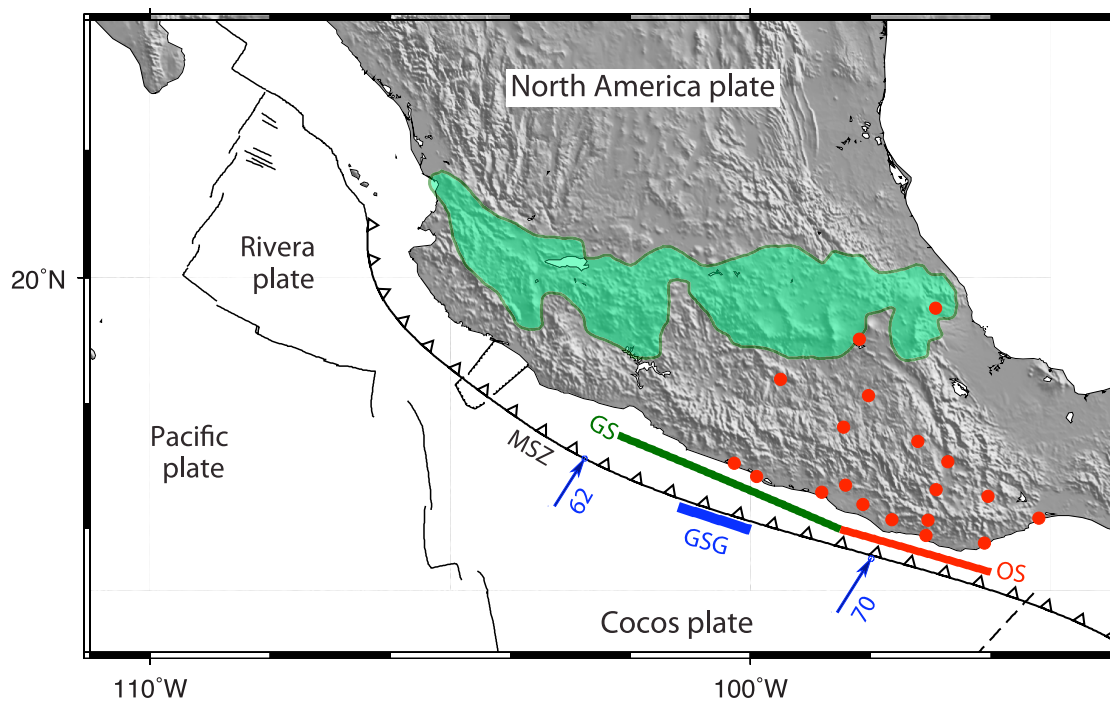


Figure 1. Regional tectonics of the study area. Convergent velocities for the Cocos Plate relative to the North America Plate are shown by blue vectors with rates in mm yr^{-1} (from DeMets *et al.* 2010). The green and red lines demarcate the along-strike limits of the Guerrero segment (GS) and Oaxaca segment (OS), respectively. The thick blue line illustrates the northwestern Guerrero seismic gap (GSG) after Radiguet *et al.* (2012). Red circles denote locations of GPS sites used to model the 2011–2012 SSE. Green area shows the Mexican Volcanic Belt. MSZ, Mexico subduction zone.

Although none of the MSZ earthquake magnitudes since 1900 have exceeded $M = 8.2$, Suarez & Albini (2009) report tsunami run-ups and modified Mercalli intensities consistent with a $M_w \sim 8.6$ earthquake that ruptured ~ 450 km of the MSZ in 1787. Moreover, calculations of synthetic seismicity for the Middle America trench based on its historic seismicity suggest an upper magnitude limit, of $M > 8$, larger than observed during the twentieth and twenty-first centuries (Ward 1991, 1992), in accord with Suarez & Albini's (2009) result.

Since the mid-1990s, cGPS receivers at an expanding number of locations in southern and central Mexico (Fig. 1) have detected SSEs along the Guerrero and Oaxaca segments of the MSZ (e.g. Kostoglodov *et al.* 2003; Brudzinski *et al.* 2007; Correa-Mora *et al.* 2008, 2009; Radiguet *et al.* 2012). Given that SSEs can load or unload stresses acting on the seismogenic zone depending on their locations on the subduction interface, significant effort is being invested into studying SSEs in Mexico.

Along the Guerrero segment, SSEs in 2001–2002, 2006 and 2009–2010 extended up-dip to 20-km depth and were characterized by large slips (~ 200 mm) and equivalent moment magnitudes of $M \sim 7.5$ (e.g. Lowry *et al.* 2001; Kostoglodov *et al.* 2003; Iglesias *et al.* 2004; Yoshioka *et al.* 2004; Larson *et al.* 2007; Radiguet *et al.* 2012; Cavalie *et al.* 2013). These SSEs, which extend ~ 250 km along-strike and reach their shallowest depths in the Guerrero seismic gap (Fig. 1), appear to have reduced the geodetic slip-rate deficit in the seismic gap to $\sim 8 \text{ mm yr}^{-1}$ from 1998 to 2010, ~ 75 per cent less than the slip-rate deficit on either side of the gap (Radiguet *et al.* 2012). This observation and the presence of SSEs beneath Guerrero may explain why no large thrust earthquake has occurred in the Guerrero seismic gap since at least 1911.

Of the 10 SSEs that have been detected along the Oaxaca segment since 1993, only those in 2004, 2006 and 2007 have been modelled prior to this study. These SSEs occurred down-dip from the rupture

zones of the most recent large earthquakes in the region in 1965 and 1978 (Fig. 2; Correa-Mora *et al.* 2008, 2009). Maximum cumulative slips were ~ 100 mm in 2004 and 2006 and had equivalent moment magnitudes of $M \sim 6.6$, significantly smaller than the SSEs beneath Guerrero. Modelling of the 2004 and 2006 SSEs and the interseismic locking that preceded both SSEs suggests that they relieved all of the elastic strain that accumulated across the deep SSE zone during the inter-SSE intervals (Correa-Mora *et al.* 2008). Unlike in Guerrero, slow slip beneath Oaxaca does not appear to intrude up-dip into the seismogenic zone (Correa-Mora *et al.* 2009).

To date, no SSE comparable to those recorded below Guerrero and Oaxaca has been detected in the region between 99°W and 98°W . More work and observations are needed to determine whether the subduction interface beneath this region differs from that below Guerrero and Oaxaca (Fig. 2) or instead merely appears to lack SSEs due to sparser GPS coverage in this region.

Tectonic tremor below southern Mexico occurs along the subduction interface down-dip from the region where SSEs occur (Fig. 2; e.g. Payero *et al.* 2008; Brudzinski *et al.* 2010) and from the hypothesized transition zone between unstable and stable sliding based on the $350\text{--}450^\circ\text{C}$ isotherms (e.g. Hyndman & Wang 1993). Below Oaxaca, tremor coincides with a region of high electrical conductivity (Jödicke *et al.* 2006), possibly caused by abundant fluids along or near the subduction interface (Song *et al.* 2009). In contrast, tremor below Guerrero does not coincide with high electrical conductivity areas (Payero *et al.* 2008). The absence of spatial overlap between SSEs and tremor suggests that the transition zone may consist of distinct zones of slow slip and deeper tremor (Brudzinski *et al.* 2010). Song *et al.* (2009) suggest that tremor is concentrated at or slightly below the 450°C isotherm, where the predicted transition from blueschist to eclogite may produce fluids that cause the observed higher electrical conductivities and possibly trigger tremor.

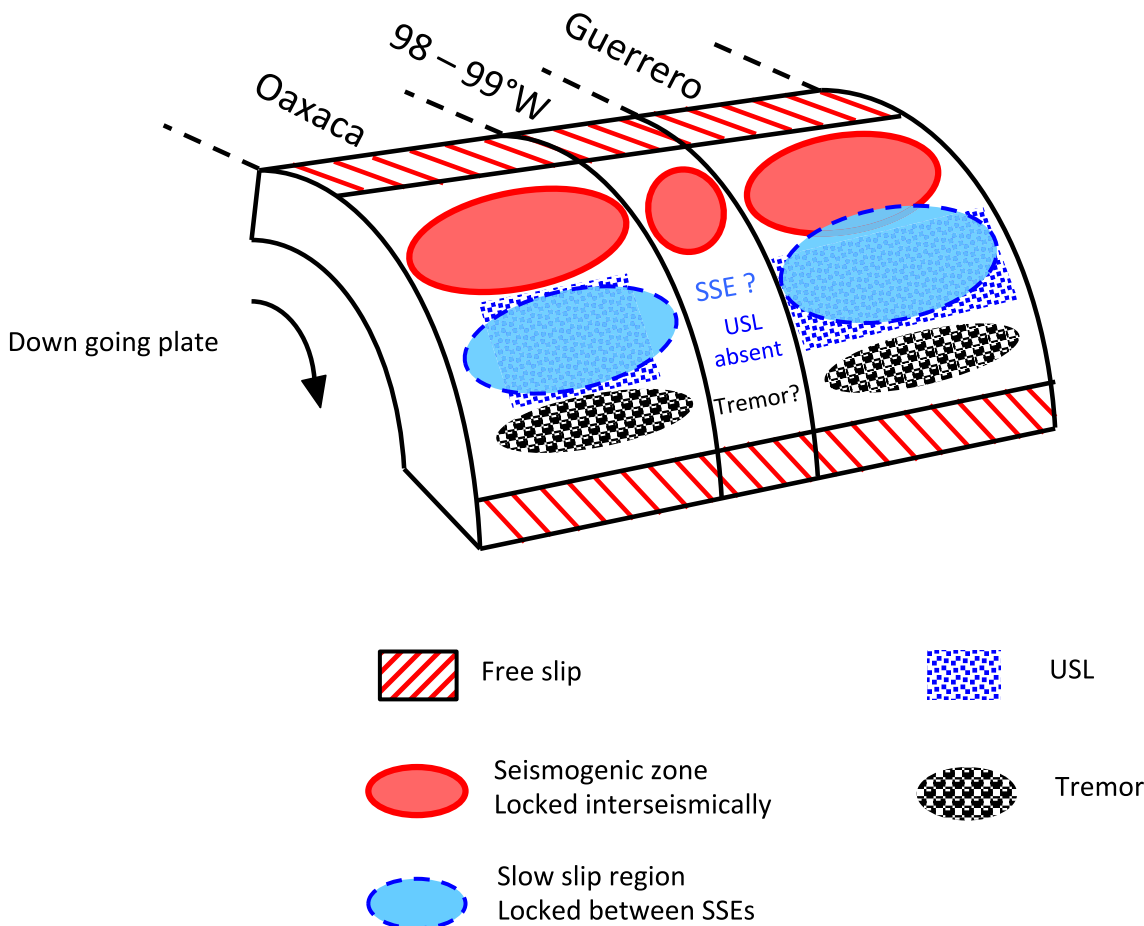


Figure 2. Seismic cycle processes and their locations on the Mexico subduction interface. USL (ultra-slow velocity layer) locations are from Song *et al.* (2009). SSE locations are from Correa-Mora *et al.* (2008) and Radiguet *et al.* (2012). Tremor locations in Oaxaca and Guerrero tremor are from Brudzinski *et al.* (2010) and Payero *et al.* (2008), respectively.

3 GPS DATA, ANALYSIS AND EXAMPLE TIME-SERIES

3.1 Data and processing methods

The data used for this analysis consist of daily 3-D position estimates at 19 cGPS stations in central and southern Mexico (Fig. 1). The stations extend ~ 300 km along the Pacific coast and ~ 450 km inland, slightly larger than the area affected by the 2011–2012 SSE. All of the GPS data were processed with Release 6.1 of the GIPSY software suite from the Jet Propulsion Laboratory (JPL). No-fiducial daily GPS station coordinates were estimated using a precise point-positioning strategy (Zumberge *et al.* 1997), including constraints on a priori tropospheric hydrostatic and wet delays from Vienna Mapping Function parameters (<http://gjosatm.hg.tuwien.ac.at>), elevation- and azimuthally dependent GPS and satellite antenna phase centre corrections from IGS08 ANTEX files (available via ftp from sideshow.jpl.nasa.gov), and corrections for ocean tidal loading (<http://holt.oso.chalmers.se>). Phase ambiguities were resolved for all the data using GIPSY's single-station ambiguity resolution feature. The no-fiducial station location estimates were transformed to IGS08 using daily seven-parameter Helmert transformations from JPL, thereby yielding daily point-positioned station coordinates that conform with ITRF08 (Altamimi *et al.* 2011).

3.2 Post-processing to reduce correlated, non-tectonic noise

Given that noise in point-positioned station coordinates remains correlated out to interstation distances of more than 3000 km (Márquez-Azúa & DeMets 2003), we applied methods described by Márquez-Azúa & DeMets (2003) to estimate the common-mode noise for stations in southern Mexico from the position time-series of more than 1000 cGPS sites located in tectonically stable areas outside of southern Mexico. As is shown in Fig. 3, applying a common-mode noise correction determined from stations outside our study area to the point-positioned daily latitudes for site OAX2 within our study area reduces by ~ 30 per cent the daily noise at OAX2, as well as reducing the amplitude of noise at periods longer than 1 d. The less noisy, corrected station time-series clearly shows the classic sawtooth-shaped SSE (Fig. 3c) and provides a strong basis for our subsequent modelling of the space-time evolution of slip on the subduction interface.

Similar corrections for common-mode noise to the daily positions at all 19 stations in our study area reduces the daily and longer period noise at all 19 stations similar to the reductions described for site OAX2. Overall, the respective rms scatters of the north, east and vertical components of the daily station positions relative to 10-d-average positions were 1.9, 2.1 and 6.1 mm before any corrections for common-mode noise. Applying the corrections reduced

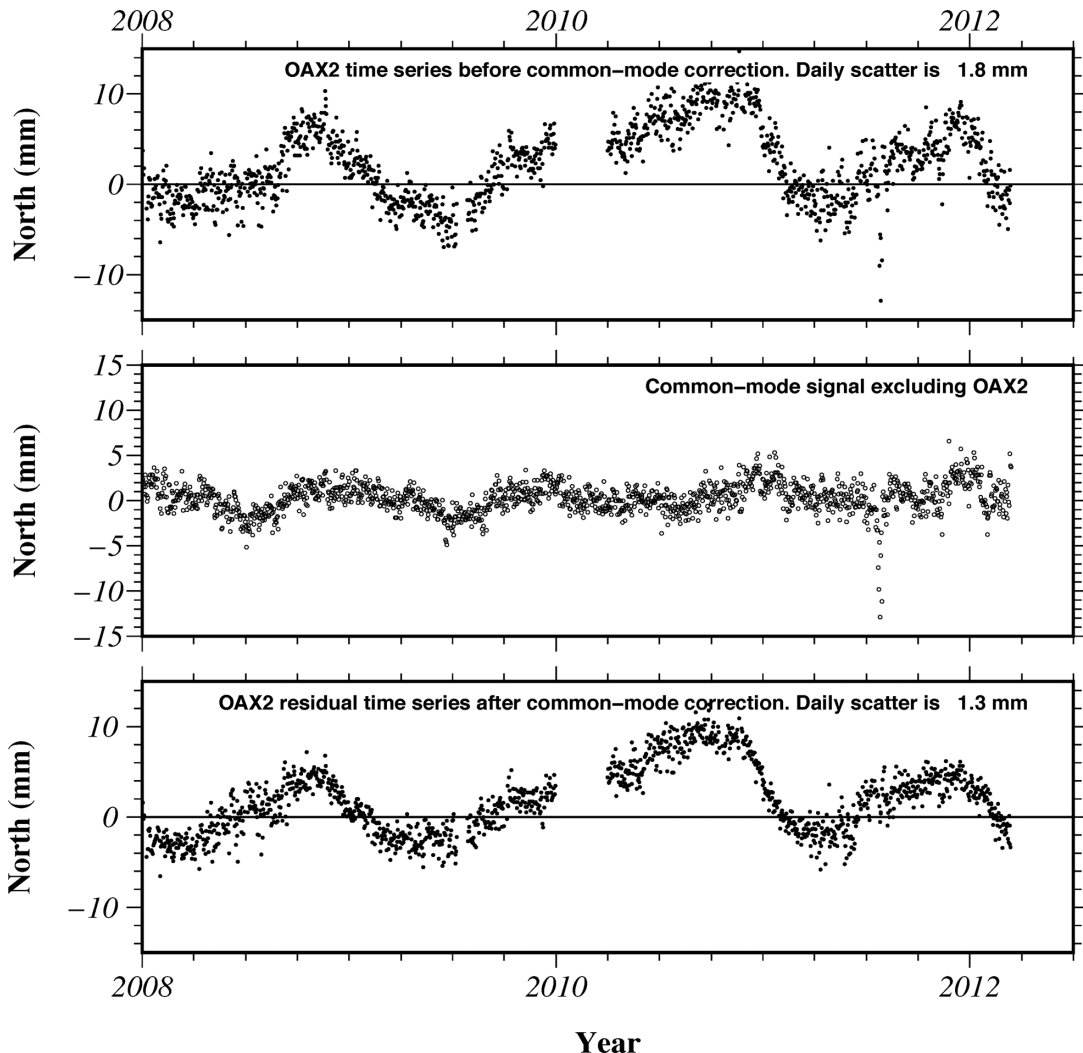


Figure 3. Effect of common-mode noise corrections to latitudinal component of the GPS time-series for site OAX2 in state of Oaxaca, Mexico. Upper panel shows daily changes in station latitude at OAX2 from GIPSY point-positioning before any correction for interstation, common-mode noise. Centre panel shows the correlated daily noise corrections (north component) determined from all continuous GPS sites within a 3000 km radius of OAX2, excluding the following: sites with time-series shorter than 2.0 yr, the OAX2 time-series, and stations with unstable motions or evidence of silent slip events. The bottom panel shows the OAX2 time-series after correcting it by the common-mode noise from the centre panel. The reduction in the $1-\sigma$ daily scatter from 1.8 to 1.3 mm improves the definition of the three SSEs that occurred during this 4-yr-long period.

the north, east and vertical rms scatters to 1.5, 1.6 and 5.7 mm, which are 24, 21, and 7 per cent smaller, respectively.

3.3 Example GPS position time-series

Fig. 4 shows an example position time-series for site OXNC, spanning ~ 7 months before and after the 2012 March 20 earthquake. Prior to early 2012, northward motion at OXNC is driven by interseismic strain accumulation from coupling across both the shallow seismogenic zone and the source region of the eventual SSE. In early 2012, the southward site motion marks the onset of slow slip along the subduction interface downdip from the seismogenic zone. On 2012 March 20, the $M_w = 7.4$ Ometepec earthquake ruptured the seismogenic zone and triggered rapid post-seismic deformation, thereby masking any continuing slow slip. After the earthquake, the motion at OXNC represents a superposition of transient post-seismic deformation, steady interseismic strain accumulation from the locked seismogenic zone and possible continued slow slip. Graham (2013) inverts cGPS data from many of the same stations

used for this analysis to model coseismic slip and afterslip for the Ometepec earthquake.

4 MODELLING METHOD: TDEFNODE

We use TDEFNODE (McCaffrey 2009) to model both the spatial and temporal evolution of slip associated with the SSE. Within TDEFNODE, simple functions are used to describe the time and space distributions of slip on the fault surface during an event as follows:

$$s(x, w, t) = AX(x)W(w)S(t), \quad (1)$$

where s is the slip rate on the fault and depends on time t and the along-strike and downdip locations x and w . The slip rate is defined as the product of the amplitude A , the along-strike and downdip components of the spatial functions $X(x)$ and $W(w)$, and the temporal function $S(t)$ (McCaffrey 2009). Elastic deformation is calculated within TDEFNODE using the Okada (1992) elastic half-space dislocation algorithm. Slip is constrained to occur on and

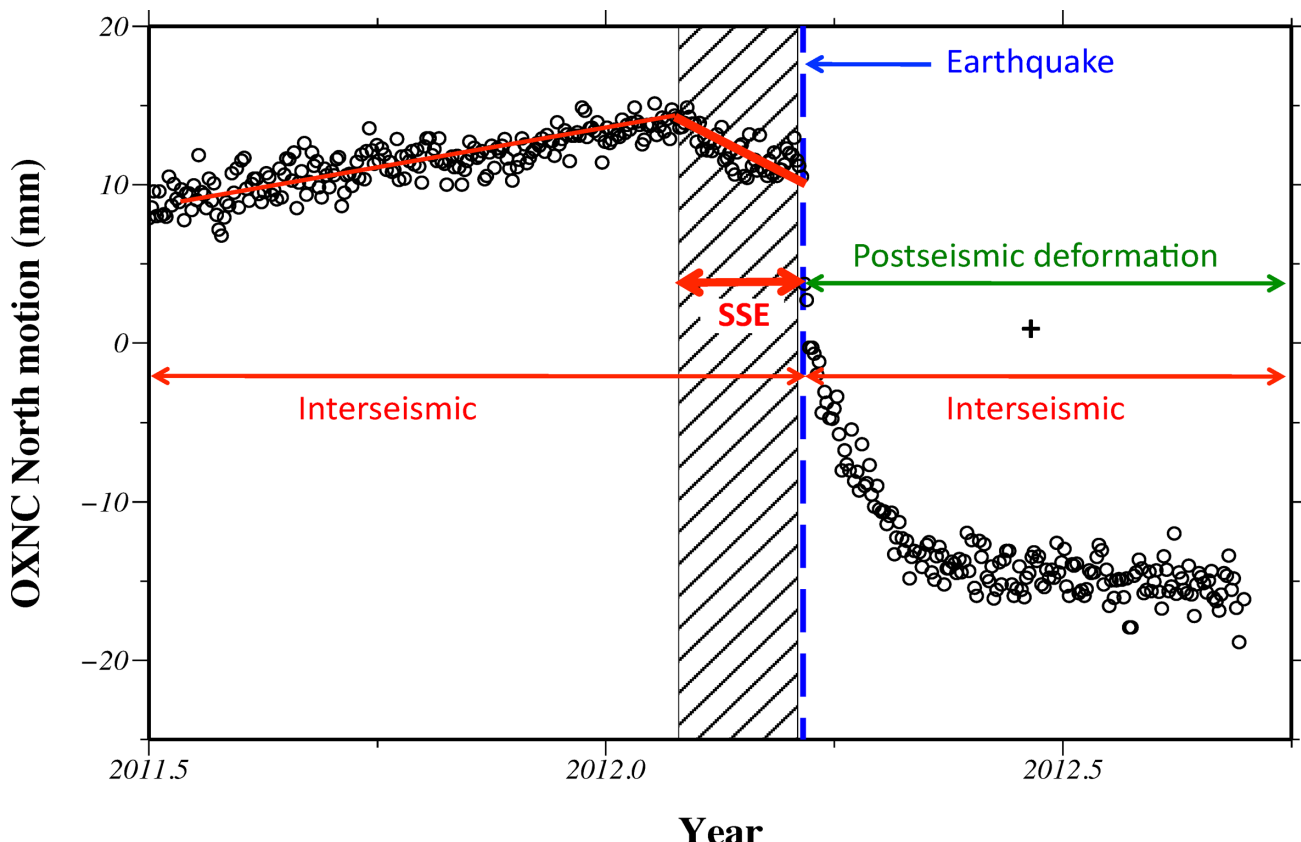


Figure 4. Time-series for north-component of motion at site OXNC illustrating interseismic strain accumulation, slow slip event (SSE), earthquake and post-seismic deformation. North America Plate motion is removed from the time-series.

tangent to the subduction interface. Estimation of the free parameters describing the source is accomplished through a combination of a grid search and simulated annealing to minimize the sum of penalties and the reduced chi-squared of the data misfit, χ^2_v , where χ^2_v is defined as χ^2/dof and degrees of freedom (dof) is equal to the number of observations minus the number of free parameters (McCaffrey 2009). Penalties are applied to constrain parameter values and to apply smoothing and damping to the slip distributions. Further details on TDEFNODE are provided in the auxiliary material of McCaffrey (2009).

Within the elastic half-space model, the subduction zone is represented using an irregular grid of node points. The node points follow depth contours from Radiguet *et al.* (2012), which in turn are based on the slab geometry of Pérez-Campos *et al.* (2008). Our model space extends along-strike from 94°W to 105°W and from the surface to 80-km depth. Fault nodes are spaced 5 km along-strike and 3 km downdip.

The GPS data used for our modelling extend from 2011 July 1, ~4 months before the start of the SSE, to the day before the Ometepec earthquake (2012 March 19). Data during the SSE are fit with (1) using fault nodes with a spread smoothing constraint, where slip is penalized for increasing distance from the slip centroid, to describe the spatial slip distribution (i.e. $X(x)$ and $W(w)$) and a Gaussian function for $S(t)$ to describe the time evolution of slip-rate per node. The parameters estimated in the inversion are the slip-rate amplitude at each node, the nominal event onset time, the rate and azimuth of slip migration, and the time constant for the Gaussian function. During the inversion, we also simultaneously solve for the inter-SSE slope of each component of the time-series for each station in order to isolate the signal of the SSE. The rake of the SSE

slip is constrained to be opposite the N32°E direction of Cocos—North America Plate convergence (DeMets *et al.* 2010).

5 SLOW SLIP PRECEDING THE 2012 MARCH EARTHQUAKE

5.1 Observational evidence for westward SSE migration

Fig. 5 summarizes evidence that the 2011–2012 SSE initiated in late 2011 near the eastern edge of the cGPS network and migrated progressively to the northwest. The SSE was first detected in early 2011 November at the two easternmost coastal and inland sites, HUAT and OXEC (Fig. 5). It was then detected at increasingly later times at stations progressively farther west and only arrived at site OMTP, the station nearest the epicentre, weeks before the earthquake. Slow slip thus migrated westward more than 300 km towards the epicentre over a period of ~130 d. In the ensuing inversion, we constrain slip migration to be generally from east to west, while allowing for up- and downdip migration, and estimate the direction and rate that the slip migrated. The cumulative surface offsets observed at the GPS sites during the SSE range from a few mm to ~10 mm (Fig. 6e), with the largest offsets near the midpoint of the cGPS network.

5.2 Best-fitting slow-slip solution

An inversion of the 19 cGPS time-series, which consist of 5326 daily north, east and vertical station positions (15 978 total), gives a best-fitting solution with slip that propagates 2.6 km per day towards N36°W from 2011 November through mid-March 2012

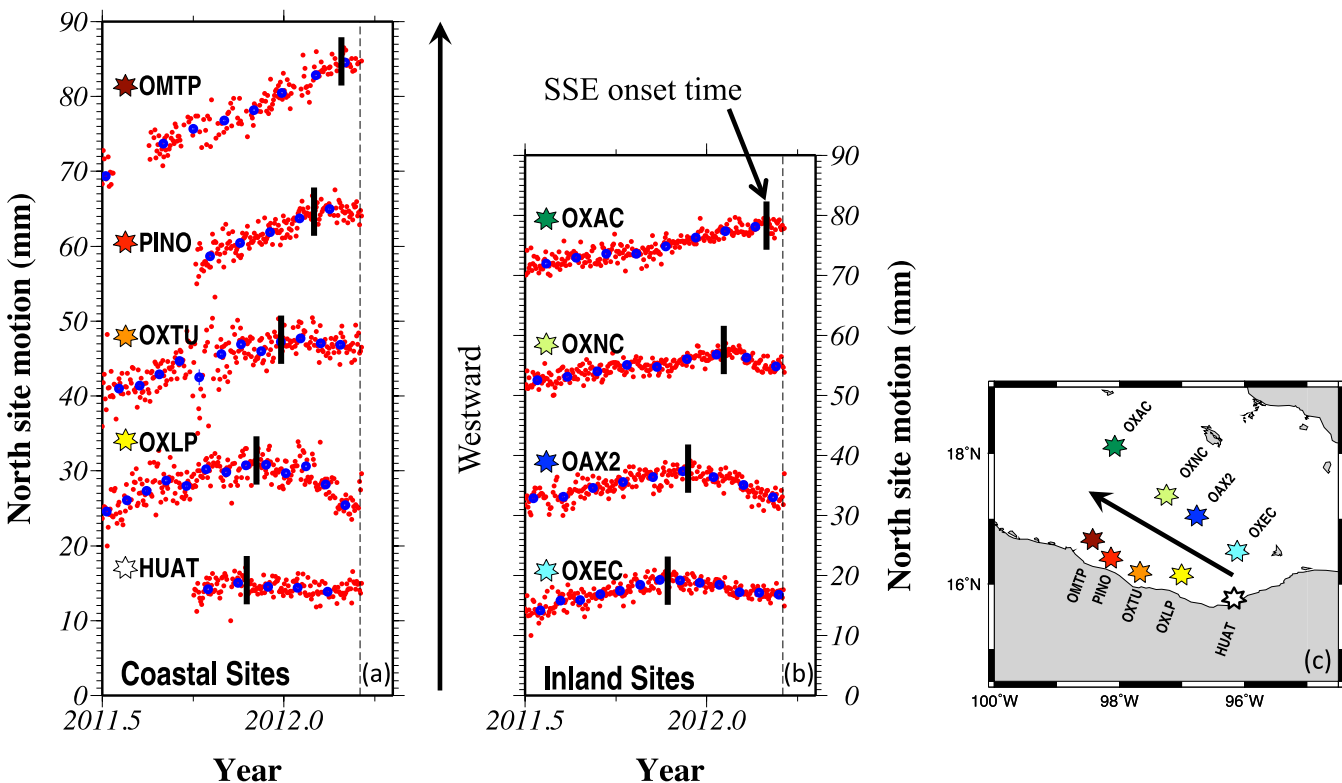


Figure 5. North component of motion for selected coastal (left) and inland (centre) GPS stations during the 2011–2012 SSE. Dashed line denotes time of the earthquake. Star and colour designates station location in the map (right). Vertical black bar indicates approximate SSE onset time. From east to west, the SSE onset times become progressively later and begin only several weeks before the Ometepec earthquake at the two westernmost sites OMTP and OXAC.

and monthly slip (Figs 6a–d) that increased in amplitude and area through early February 2012. After early February of 2012, the SSE amplitude decayed until the 2012 March 20 earthquake and its afterslip masked the much smaller-magnitude slow slip. During the month preceding the earthquake, modest amounts of slow slip (<20 mm) migrated to the region located downdip from the eventual rupture zone (Fig. 6d). Evidence for this consists of small-magnitude transient motions that were recorded at sites PINO, OMTP and MRQL at the western edge of the study area (Fig. A1).

The GPS station motions estimated from the above slip solution correctly match the observed SSE onset times, durations and offset amplitudes (Figs 7 and A1). The WRMS (weighted root mean square) misfit to the 19 cGPS time-series is 2.2 mm, close to the observed scatter in the daily station positions. Encouragingly, the cumulative, observed vector offsets, during the SSE of the 19 cGPS sites (shown by the white arrows in Fig. 6e) are well matched by the offsets estimated from the best-fitting, time-dependent slip solution (red arrows in Fig. 6e). The cumulative slip solution (Fig. 6e) has a maximum slip amplitude of ~100 mm near 97°W at 30-km depth and slip of only 5–10 mm near the eventual earthquake rupture zone. If we enforce zero slip for areas of the subduction interface near the earthquake rupture zone, the small motions at sites MRQL and OMTP near the eventual earthquake rupture zone are not fit (Fig. 7). The total moment released for the SSE was 3.0×10^{19} N·m ($M_w = 6.9$), assuming a shear modulus of 30 GPa and a Poisson's ratio of 0.25, comparable to the 2004 and 2006 SSEs in the same area (Correa-Mora *et al.* 2008). Most slip is focused between the 20 and 40 km subduction depth contours, consistent with previously reported SSE depths for Oaxaca (Correa-Mora *et al.* 2008, 2009).

5.3 Slow slip: model uncertainties and alternative models

We evaluated a range of smoothing methods and smoothing factors to determine the trade-off between the misfits and the complexity of the predicted slip solutions (Fig. 8). We find that a spread smoothing parameterization, which penalizes solutions that spread slip over a broad region, works best. As expected, slip solutions with smaller smoothing factors become increasingly complex and include more slip at the eastern and western ends of the SSE, farther from the SSE centroid (e.g. Fig. 8a). Conversely, as smoothing is increased and slip is therefore encouraged to occur within a smaller area, the slip becomes more concentrated and its amplitude increases (e.g. Fig. 8c). The maximum slip in the oversmoothed model depicted in Fig. 8(c) is 210 mm, double that of the preferred model (Fig. 8b). The good fits to the high-displacement GPS sites such as OXEC and OXGU (Fig. 7) are relatively unaffected by changes in the smoothing parameter and thus provide little information about what the best smoothing factor might be. Instead, we use misfits to the GPS sites near the edges of the network to determine how much smoothing to use. The preferred solution (Fig. 8b) represents the most smoothing that can be applied before the misfits at the peripheral GPS stations increase significantly. Although the preferred slip solution includes slip as small as 5 mm along the edges of the SSE, it is unlikely that such slip is well resolved. None of our subsequent results or conclusions, including the Coulomb stress calculations, depend on slip values smaller than 10 mm.

The SSE depth range of 20–40 km is a robust feature of the slip solutions, depending little or not at all on the magnitude or type of smoothing we used for a particular inversion. A less robust, but nonetheless important feature of the slip solutions is the zone of slip

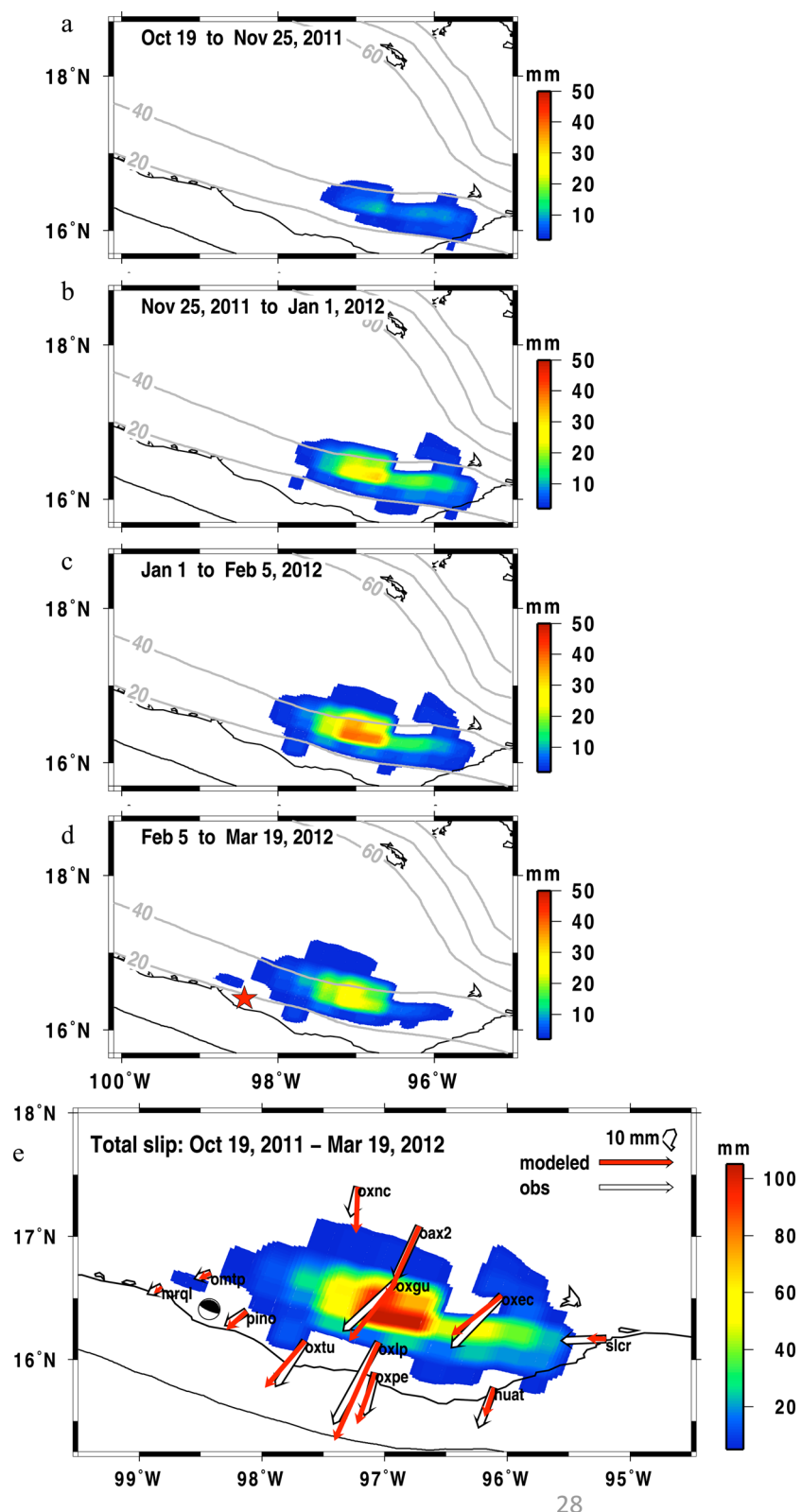


Figure 6. (a)–(d) Best-fitting slow slip solution at ~monthly intervals late 2011 October to 2012 March 19. (e) Total slip from late 2011 October to 2012 March 19 for preferred slow slip model. Predicted offsets for this slip distribution are shown as red arrows and observed overall offsets as white arrows. Focal mechanism is for the 2012 March 20 earthquake (from the Global CMT catalogue <http://www.globalcmt.org>). Subduction depth contours from Radiguet *et al.* (2012).

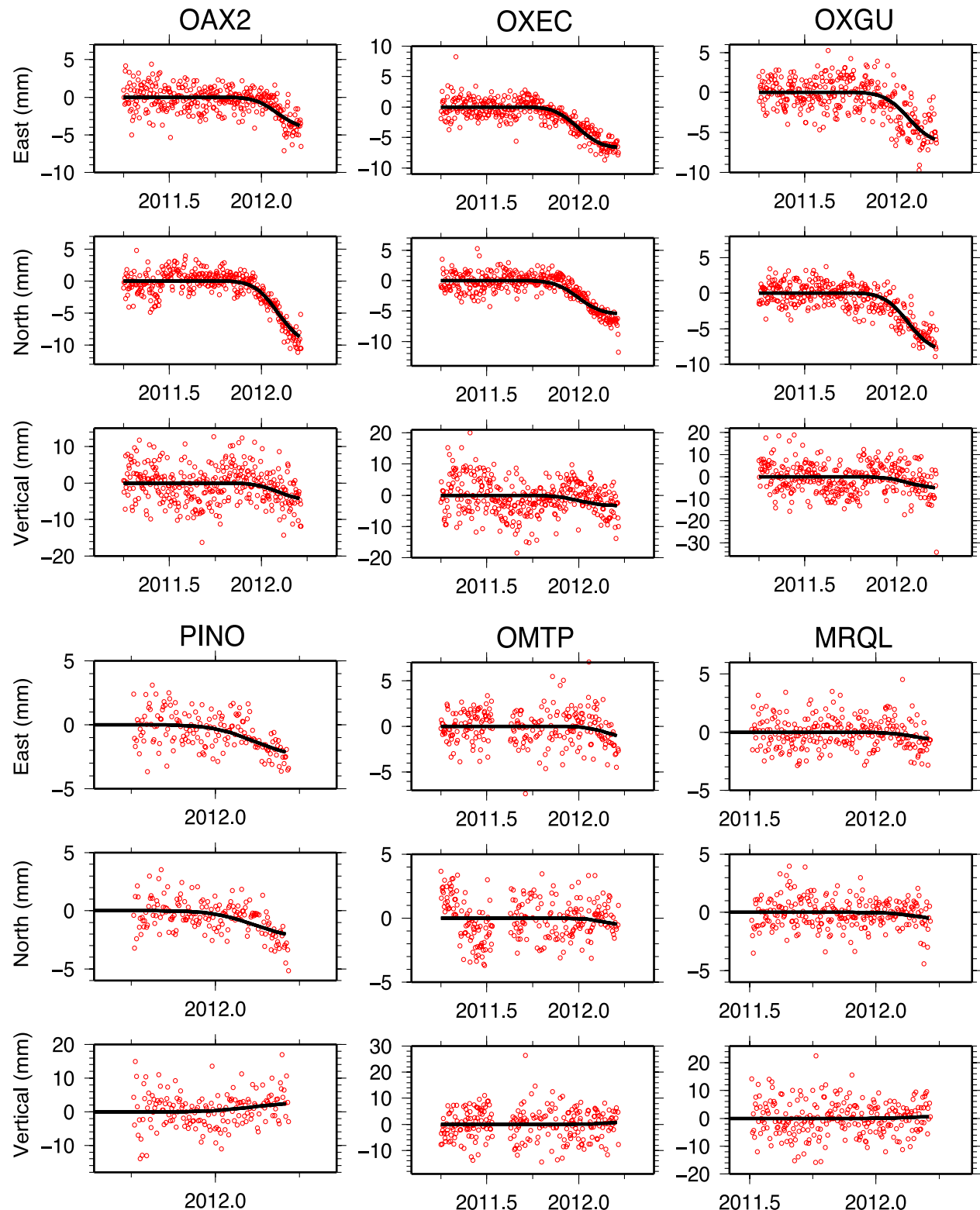


Figure 7. Observed versus modelled GPS time-series from the preferred slow slip solution. Red circles show daily station positions reduced by the best-fitting slope from 2011 May through SSE onset time. Black line shows predictions for the preferred slip solution. Station names are given above each set of east, north and vertical displacements (top middle and bottom, respectively). Fits to all 19 station time-series are given in Fig. A1.

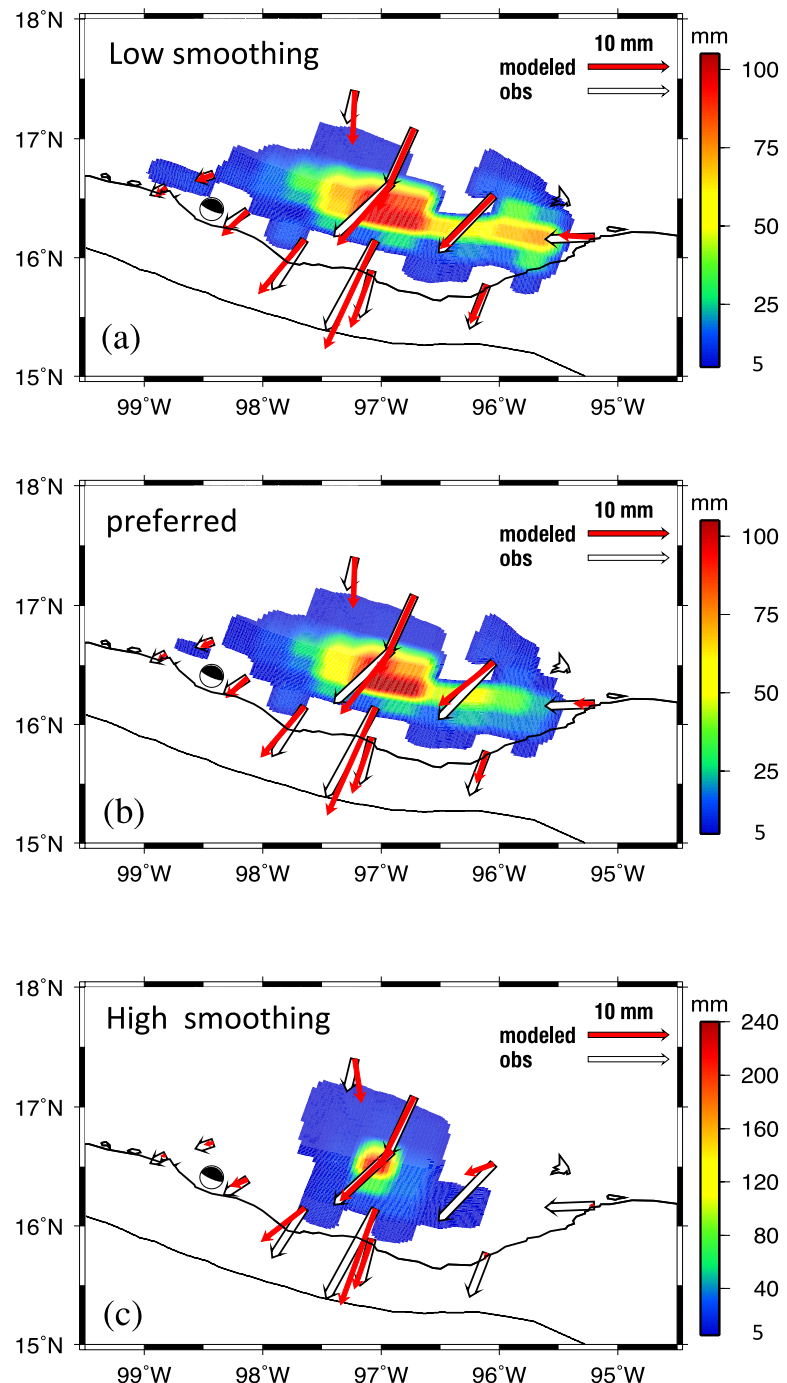


Figure 8. Effects of smoothing on the SSE model. (a) Less smoothing than preferred model (b), and (c) more smoothing than preferred model. The largest changes in fit come at the stations located on the eastern and western edges of the network. Note that (c) has a different scale. Focal mechanism denotes location of the 2012 March 20 $M_w = 7.4$ Ometepec earthquake (from USGS).

that protrudes westward to 98°W – 98.5°W (Fig. 6e), immediately down-dip from the Ometepec rupture zone. Models that preclude any slip in this region fail to fit the time-series for sites OMTP and MRQL west of the earthquake epicentre. The GPS data thus strongly suggest that the SSE extended nearly 300 km along-strike.

6 COULOMB STRESS CALCULATIONS

Positive static Coulomb stress changes (CSCs) as a result of earthquake slip have been correlated to regions of aftershocks, suggesting

that increased stresses can trigger aftershocks (e.g. Toda *et al.* 1998). This relationship implies that a SSE may alter stresses enough to trigger a large thrust earthquake. The spatial-temporal proximity between the SSE and the Ometepec earthquake is consistent with such a relationship. In order to determine the impact of the 2011–2012 SSE on the seismogenic zone, we calculated the CSC using our preferred slip solution. Given that the CSC is dependent on the slip solution and can be sensitive to small changes in slip, we determined CSC for using only areas of the fault with SSE slip greater than 30 (Fig. 9a), 10 (Fig. 9b) and 5 mm (Fig. 9c). CSCs are

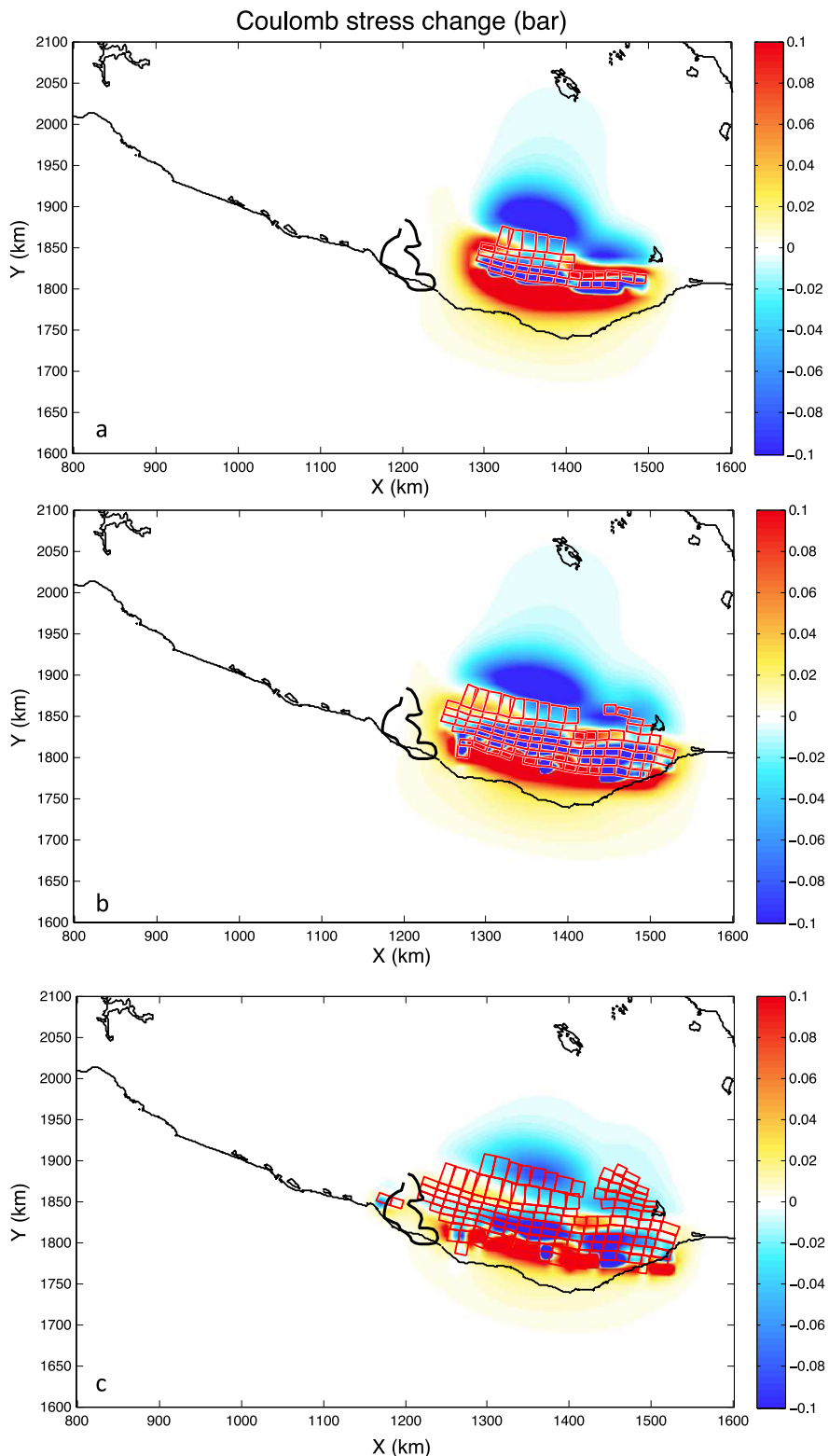


Figure 9. Coulomb stress change calculations for slip during the 2011–2012 SSE based on (a) slip 30 mm and greater, (b) slip 10 mm and greater (c) slip 5 mm and greater. Red boxes indicate fault patches used in the calculation. Black outline is the geodetic slip source region for the Ometepec earthquake from Graham (2013).

calculated with Coulomb 3.3 (Lin & Stein 2004; Toda *et al.* 2005) with an effective coefficient of friction to 0.4 and a strike, dip and depth consistent with the fault at seismogenic depths. Changing the effective coefficient of friction to 0.2, corresponding to higher pore

fluid pressures, does not significantly change the results, that is the location of positive and negative CSC.

For slip greater than or equal to 30 mm (Fig. 9a), positive CSCs do not reach the geodetically determined earthquake source region

as defined by Graham (2013). Positive CSCs of a few to 10 kPa (0.1 bar) in the region of earthquake slip are, however, predicted if slow slip equal to or greater than 10 mm is also included in the calculation (Fig. 9b). Even larger positive stress changes are predicted for solutions that are driven using slip as small as 5 mm (Fig. 9c), although slip values this small may not be well resolved and are not required to generate CSCs that encourage rupture at the vicinity of the eventual 2012 March 20 earthquake.

7 DISCUSSION

7.1 Comparison to previous SSEs

All four SSEs in this region with published slip solutions (Fig. 10) have been focused between 96°W and 98°W, have maximum slip at ~97°W, and occurred downdip from the seismogenic zone. The

maximum slip amplitudes in 2004, 2006 and 2011–2012 were ~100 mm, but were smaller in 2007 (~30 mm). Our results suggest that the 2011–2012 Oaxaca SSE extended farther west towards Guerrero than was the case for previous SSEs (Fig. 10) and included little or no slip from 99°W to 98°W, where no SSE has yet been recorded. Although slow slip that originated beneath Guerrero in 2001 may have migrated as far east as 97°W (Radiguet *et al.* 2012), the absence of any GPS stations between 100°W and 98°W in 2001 leaves open the question of whether slow slip migrated across the 99°W–98°W gap. Relatively new GPS stations that are now operating between 99°W and 98°W will help resolve whether the subduction interface in this region accommodates SSE or is instead a gap for reasons not yet understood.

7.2 Relationship of the 2011–2012 SSE to the Ometepec earthquake

Our modelling results suggest that small-magnitude slow slip (~5–10 mm) migrated to a location near the Ometepec earthquake source region in the weeks before the rupture. CSC calculations further indicate that small but positive stress increases occurred on the subduction zone within the source region of the Ometepec earthquake. Though small, the predicted 1–10 kPa stress changes are comparable to dynamic stresses produced by passing surface waves, which are known to trigger tectonic tremor (e.g. Peng *et al.* 2009; Rubinstein *et al.* 2009; Fry *et al.* 2011). The sequence of events whereby a slow CSC might trigger a large thrust earthquake is unclear; however, ongoing work on micro-earthquakes that occurred in the region between the 2011–2012 SSE and the Ometepec earthquake rupture zone in the weeks prior to the main shock (Sit 2013) may shed further light on this topic.

Although we cannot demonstrate causality, our results are consistent with the hypothesis that the 2011–2012 Oaxaca SSE triggered the Ometepec earthquake. In light of evidence described by Ito *et al.* (2012) for an SSE on the Japan subduction interface prior to a $M_w = 6.1$ earthquake in 2008 and for slow slip on the Japan subduction interface prior to the 2011 $M_w = 9.0$ Tohoku-Oki earthquake and its $M_w = 7.3$ foreshock (Kato *et al.* 2012), we briefly discuss whether the occurrence of SSE along the MSZ may be a useful criterion for seismic forecasting.

Since 1993, when cGPS measurements began in southern Mexico, two large thrust earthquakes have occurred—the 1995 September $M_w = 7.3$ Copala earthquake and the 2012 $M_w = 7.4$ Ometepec earthquake. No apparent SSE occurred before the 1995 Copala earthquake (see fig. 5 of Márquez-Azúa & DeMets 2009), whereas the Ometepec earthquake was associated in space and time with the SSE modelled in this study. During this same time interval, at least 15 SSEs have occurred on the Guerrero and Oaxaca segments of the MSZ. Along the more steeply dipping Rivera Plate subduction interface at the NW end of the MSZ, where no SSE has been recorded since the initiation of GPS observations in 1993, neither the 1995 October $M_w = 8.0$ Colima-Jalisco earthquake nor the 2003 January $M_w = 7.6$ Tecoman earthquake were preceded by a SSE (see fig. 13 in Schmitt *et al.* 2007 and fig. 8 in Márquez-Azúa & DeMets 2009).

The evidence thus shows that large MSZ thrust earthquakes are not inevitably preceded by slow slip, but that one of the ~15 SSEs in southern Mexico during the past two decades may have triggered a large thrust earthquake. Incorporating SSEs into seismic forecasts thus seems warranted, but will be challenging. Furthermore, slow slip appears to affect stresses across the seismogenic zone differently along the MSZ. Along the Guerrero seismic gap, SSEs

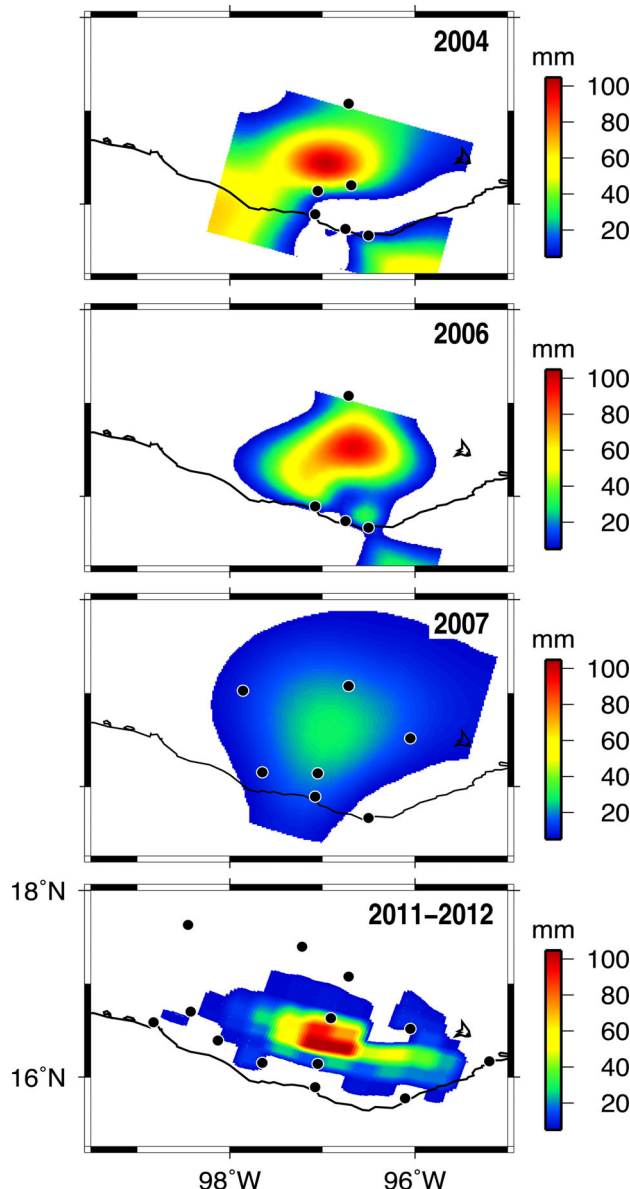


Figure 10. Slip solutions for SSEs in 2004, 2006 (Correa-Mora *et al.* 2008) and 2007 (Correa-Mora *et al.* 2009) compared to that for the 2011–2012 SSE. Black circles indicate locations of cGPS stations used to determine each slip solution.

extend updip to seismogenic depths and appears to relieve stresses that accumulate across the seismogenic zone (Radiguet *et al.* 2012; Cavalie *et al.* 2013). In contrast, SSEs along the Oaxaca segment are confined to deeper source regions and load the seismogenic zone (Correa-Mora *et al.* 2008).

Recent modelling reinforces the difficulty of incorporating SSEs into earthquake forecast models. From quasi-dynamic 2-D simulations of slip along subduction interfaces that incorporate rate-state variable friction behaviour, dilatancy and coupled 1-D pore-fluid and heat transport, Segall & Bradley (2012) find that repeated SSEs may trigger earthquakes via at least two mechanisms. One concentrates stresses at the lower limit of the locked zone, eventually leading to eventual SSE penetration of the locked zone and dynamic rupture. The other proposed mechanism enhances SSE length and slip speed with time, ultimately nucleating dynamic rupture of the SSE region that propagates updip. In both cases, the SSE that ultimately triggers the earthquake is indistinguishable from those that preceded it, although the time dependence built into their model increases the potential triggering effect of SSEs later in the cycle relative to successively earlier SSEs.

In light of the above, efforts to incorporate SSEs into forecast scenarios for earthquakes along the MSZ might include periodically updated models of the evolution of stress for known rupture zones along the MSZ, particularly where SSEs are thought to load the downdip edge of the seismogenic zone. Timely detection and location of SSE via real-time cGPS monitoring are essential elements of such forecasting, particularly since much of the frequent non-volcanic tremor recorded beneath southern Mexico does not correlate in space or time with slow slip (Brudzinski *et al.* 2010; Kostoglodov *et al.* 2010) and thus cannot be used as a seismological proxy for SSEs.

8 CONCLUSIONS

Modelling of cGPS observations from southern Mexico in 2011–2012 shows that slow slip initiated on the subduction interface below eastern Oaxaca in 2011 November and by mid-March 2012 had migrated close to the eventual rupture zone of the 2012 March 20 $M_w = 7.4$ Ometepec earthquake. The SSE caused small but positive CSCs in the earthquake source region, supporting the hypothesis that the SSE (or micro-seismicity associated with it) triggered the Ometepec earthquake. The SSE had a maximum slip amplitude of ~ 100 mm and cumulative moment release of 3.0×10^{19} N·m ($M_w = 6.9$). The SSE magnitude and its location downdip from the seismogenic zone are both similar to previous SSEs below Oaxaca.

ACKNOWLEDGEMENTS

Funding was provided in part by National Science Foundation grant EAR-1114174 (DeMets). Graphics were prepared with Generic Mapping Tools software (Wessel & Smith 1991). Portions of the GPS network were supported by the CONACYT 84544, PAPIIT IN110611 grants (Mexico) and by the Agence Nationale de la Recherche (France) under the contract RA0000CO69 (G-GAP). We thank Laura Wallace and one anonymous reviewer for their helpful comments and suggestions.

REFERENCES

- Altamimi, Z., Collilieux, X. & Métivier, L., 2011. ITRF2008: an improved solution of the international terrestrial reference frame, *J. Geodyn.*, **85**, 457–473.
- Anderson, J.G., Singh, S.K., Espindola, J.M. & Yamamoto, J., 1989. Seismic strain release in the Mexican subduction thrust, *Phys. Earth planet. Inter.*, **58**, 307–322.
- Brudzinski, M., Cabral-Cano, E., Correa-Mora, F., DeMets, C. & Márquez-Azúa, B., 2007. Slow slip transients along the Oaxaca subduction segment from 1993 to 2007, *Geophys. J. Int.*, **171**, 523–538.
- Brudzinski, M.R., Hinojosa-Prieto, H.R., Schlanser, K.M., Cabral-Cano, E., Arciniega-Ceballos, A., Diaz-Molina, O. & DeMets, C., 2010. Non-volcanic tremor along the Oaxaca segment of the Middle America subduction zone, *J. geophys. Res.: Solid Earth*, **115**, B00A23, doi:10.1029/2008JB006061.
- Cavalie, O., Pathier, E., Radiguet, M., Vergnolle, M., Cotte, N., Walpersdorf, A., Kostoglodov, V. & Cotton, F., 2013. Slow slip event in the Mexican subduction zone: evidence of shallower slip in the Guerrero seismic gap for the 2006 event revealed by the joint inversion of InSAR and GPS data, *Earth planet. Sci. Lett.*, **367**, 52–60.
- Correa-Mora, F., DeMets, C., Cabral-Cano, E., Diaz-Molina, O. & Marquez-Azua, B., 2009. Transient deformation in southern Mexico in 2006 and 2007: evidence for distinct deep-slip patches beneath Guerrero and Oaxaca, *Geochem. Geophys. Geosyst.*, **10**, Q02S12, doi:10.1029/2008GC002211.
- Correa-Mora, F., DeMets, C., Cabral-Cano, E., Marquez-Azua, B. & Diaz-Molina, O., 2008. Interplate coupling and transient slip along the subduction interface beneath Oaxaca, Mexico, *Geophys. J. Int.*, **175**, 269–290.
- DeMets, C., Gordon, R.G. & Argus, D.F., 2010. Geologically current plate motions, *Geophys. J. Int.*, **181**, 1–80.
- Dragert, H., Wang, K. & James, T.S., 2001. A silent slip event on the deeper Cascadia subduction interface, *Science*, **292**, 1525–1528.
- Fry, B., Chao, K., Bannister, S., Peng, Z. & Wallace, L., 2011. Deep tremor in New Zealand triggered by the 2010 M_w 8.8 Chile earthquake, *Geophys. Res. Lett.*, **38**, L15306, doi:10.1029/2011GL048319.
- Graham, S.E., 2013. Earthquake cycle deformation in Mexico and Central America constrained by GPS: implications for coseismic, postseismic, and slow slip, *Doctoral dissertation (Geophysics)*, University of Wisconsin, Madison.
- Hyndman, R.D. & Wang, K., 1993. Thermal constraints on the zone of major thrust earthquake failure: the Cascadia Subduction Zone, *J. geophys. Res.: Solid Earth*, **98**, 2039–2060.
- Iglesias, A., Singh, S., Lowry, A., Santoyo, M., Kostoglodov, V., Larson, K., Franco-Sánchez, S. & Mikumo, T., 2004. The silent earthquake of 2002 in the Guerrero seismic gap, Mexico ($M_w = 7.6$): inversion of slip on the plate interface and some implications, *Geof. Int.-Mexico*, **43**, 309–317.
- Ito, Y. *et al.*, 2012. Episodic slow slip events in the Japan subduction zone before the 2011 Tohoku-Oki earthquake. *Tectonophysics*, **600**, doi:10.1016/j.tecto.2012.08.022.
- Jödicke, H., Jordig, A., Ferrari, L., Arzate, J., Mezger, K. & Rüpke, L., 2006. Fluid release from the subducted Cocos plate and partial melting of the crust deduced from magnetotelluric studies in southern Mexico: implications for the generation of volcanism and subduction dynamics, *J. geophys. Res.: Solid Earth*, **111**, B08102, doi:10.1029/2005JB003739.
- Kato, A., Obara, K., Igarashi, T., Tsuruoka, H., Nakagawa, S. & Hirata, N., 2012. Propagation of slow slip leading up to the 2011 M_w 9.0 Tohoku-Oki earthquake, *Science*, **335**, 705–708.
- Kostoglodov, V., Husker, A., Shapiro, N.M., Payero, J.S., Campillo, M., Cotte, N. & Clayton, R., 2010. The 2006 slow slip event and nonvolcanic tremor in the Mexican subduction zone, *Geophys. Res. Lett.*, **37**, L24301, doi:10.1029/2010GL045424.
- Kostoglodov, V., Singh, S.K., Santiago, J.A., Franco, S.I., Larson, K.M., Lowry, A.R. & Bilham, R., 2003. A large silent earthquake in the Guerrero seismic gap, Mexico, *Geophys. Res. Lett.*, **30**, 1807, doi:10.1029/2003GL017219.
- Larson, K.M., Kostoglodov, V., Miyazaki, S.I. & Santiago, J.A.S., 2007. The 2006 aseismic slow slip event in Guerrero, Mexico: new results from GPS, *Geophys. Res. Lett.*, **34**, L13309, doi:10.1029/2007GL029912.
- Lin, J. & Stein, R.S., 2004. Stress triggering in thrust and subduction earthquakes, and stress interaction between the southern San Andreas and nearby thrust and strike-slip faults, *J. geophys. Res.*, **109**, B02303, doi:10.1029/2003JB002607.

- Lowry, A., Larson, K., Kostoglodov, V. & Bilham, R., 2001. Transient fault slip in Guerrero, southern Mexico, *Geophys. Res. Lett.*, **28**, 3753–3756.
- Márquez-Azúa, B. & DeMets, C., 2003. Crustal velocity field of Mexico from continuous GPS measurements, 1993 to June 2001: implications for the neotectonics of Mexico, *J. geophys. Res.: Solid Earth*, **108**, 2450, doi:10.1029/2002JB002241.
- Márquez-Azúa, B. & DeMets, C., 2009. Deformation of Mexico from continuous GPS measurements from 1993 to 2008, *Geochem. Geophys. Geosys.*, **10**, doi:10.1029/2008GC002278.
- McCaffrey, R., 2009. Time-dependent inversion of three-component continuous GPS for steady and transient sources in northern Cascadia, *Geophys. Res. Lett.*, **36**, L07304, doi:10.1029/2008GL036784.
- Okada, Y., 1992. Internal deformation due to shear and tensile faults in a half-space, *Bull. Seism. Soc. Am.*, **82**, 1018–1040.
- Payero, J.S., Kostoglodov, V., Shapiro, N., Mikumo, T., Iglesias, A., Pérez-Campos, X. & Clayton, R.W., 2008. Nonvolcanic tremor observed in the Mexican subduction zone, *Geophys. Res. Lett.*, **35**, L07305, doi:10.1029/2007GL032877.
- Peng, Z., Vidale, J., Wech, A., Nadeau, R. & Creager, K., 2009. Remote triggering of tremor along the San Andreas Fault in central California, *J. geophys. Res.*, **114**, B00A06, doi:10.1029/2008JB006049.
- Pérez-Campos, X. et al., 2008. Horizontal subduction and truncation of the Cocos Plate beneath central Mexico, *Geophys. Res. Lett.*, **35**, L18303, doi:10.1029/2008GL035127.
- Radiguet, M., Cotton, F., Vergnolle, M., Campillo, M., Walpersdorf, A., Cotte, N. & Kostoglodov, V., 2012. Slow slip events and strain accumulation in the Guerrero gap, Mexico, *J. geophys. Res.: Solid Earth*, **117**, B04305, doi:10.1029/2011JB008801.
- Rubinstein, J.L., Gomberg, J., Vidale, J.E., Wech, A.G., Kao, H., Creager, K.C. & Rogers, G., 2009. Seismic wave triggering of nonvolcanic tremor, episodic tremor and slip, and earthquakes on Vancouver Island, *J. geophys. Res.*, **114**, B00A01, doi:10.1029/2008JB005875.
- Schmitt, S.V., DeMets, C., Stock, J., Sanchez, O., Marquez-Azua, B. & Reyes, G., 2007. A geodetic study of the 2003 January 22 Tecoman, Colima, Mexico earthquake, *Geophys. J. Int.*, **169**, 389–406.
- Schwartz, S.Y. & Rokosky, J.M., 2007. Slow slip events and seismic tremor at circum-Pacific subduction zones, *Rev. Geophys.*, **45**, RG3004, doi:10.1029/2006RG000208.
- Segall, P. & Bradley, A.M., 2012. Slow-slip evolves into megathrust earthquakes in 2D numerical simulations, *Geophys. Res. Lett.*, **39**, L18308, doi:10.1029/2012GL052811.
- Singh, S.K., Astiz, L. & Havskov, J., 1981. Seismic gaps and recurrence periods of large earthquakes along the Mexican subduction zone: a reexamination, *Bull. seism. Soc. Am.*, **71**, 827–843.
- Sit, S.M., 2013. New methods in geophysics and science education to analyze slow fault slip and promote active e-learning, *Doctoral dissertation (Geology)*, Miami University.
- Song, T.-R.A., Helmberger, D.V., Brudzinski, M.R., Clayton, R.W., Davis, P., Pérez-Campos, X. & Singh, S.K., 2009. Subducting slab ultra-slow velocity layer coincident with silent earthquakes in southern Mexico, *Science*, **324**, 502–506.
- Suarez, G. & Albini, P., 2009. Evidence for great tsunamigenic earthquakes (M 8.6) along the Mexican subduction zone, *Bull. seism. Soc. Am.*, **99**, 892–896.
- Toda, S., Stein, R.S., Reasenberg, A., Dieterich, J.H. & Yoshida, A., 1998. Stress transferred by the 1995 $M_w = 6.9$ Kobe, Japan shock: effect on aftershocks and future earthquake probabilities, *J. geophys. Res.*, **103**, 24 543–24 565.
- Toda, S., Stein, R.S., Richards-Dinger, K. & Bozkurt, S., 2005. Forecasting the evolution of seismicity in southern California: animations built on earthquake stress transfer, *J. geophys. Res.*, **110**, B05S16, doi:10.1029/2004JB003415.
- Universidad Nacional Autónoma de México Seismology Group, 2013. Ometepec-Pinotepa Nacional, Mexico earthquake of 20 March 2012 (M_w 7.5): a preliminary report, *Geofísica Internacional*, **52–2**, 173–196.
- Ward, S.N., 1991. A synthetic seismicity model for the Middle America trench, *J. geophys. Res.*, **96**, 21 433–21 442.
- Ward, S.N., 1992. An application of synthetic seismicity in earthquake statistics: the Middle America trench, *J. geophys. Res.*, **97**, 6675–6682.
- Wessel, P. & Smith, W.H.F., 1991. Free software helps map and display data, *EOS, Trans. Am. geophys. Un.*, **72**, 455–473.
- Yoshioka, S., Mikumo, T., Kostoglodov, V., Larson, K.M., Lowry, A.R. & Singh, S.K., 2004. Interplate coupling and a recent aseismic slow slip event in the Guerrero seismic gap of the Mexican subduction zone, as deduced from GPS data inversion using a Bayesian information criterion, *Phys. Earth planet. Inter.*, **146**, 513–530.
- Zumberge, J.F., Heflin, M.B., Jefferson, D.C., Watkins, M.M. & Webb, F.H., 1997. Precise point positioning for the efficient and robust analysis of GPS data from large networks, *J. geophys. Res.: Solid Earth*, **102**, 5005–5017.

APPENDIX

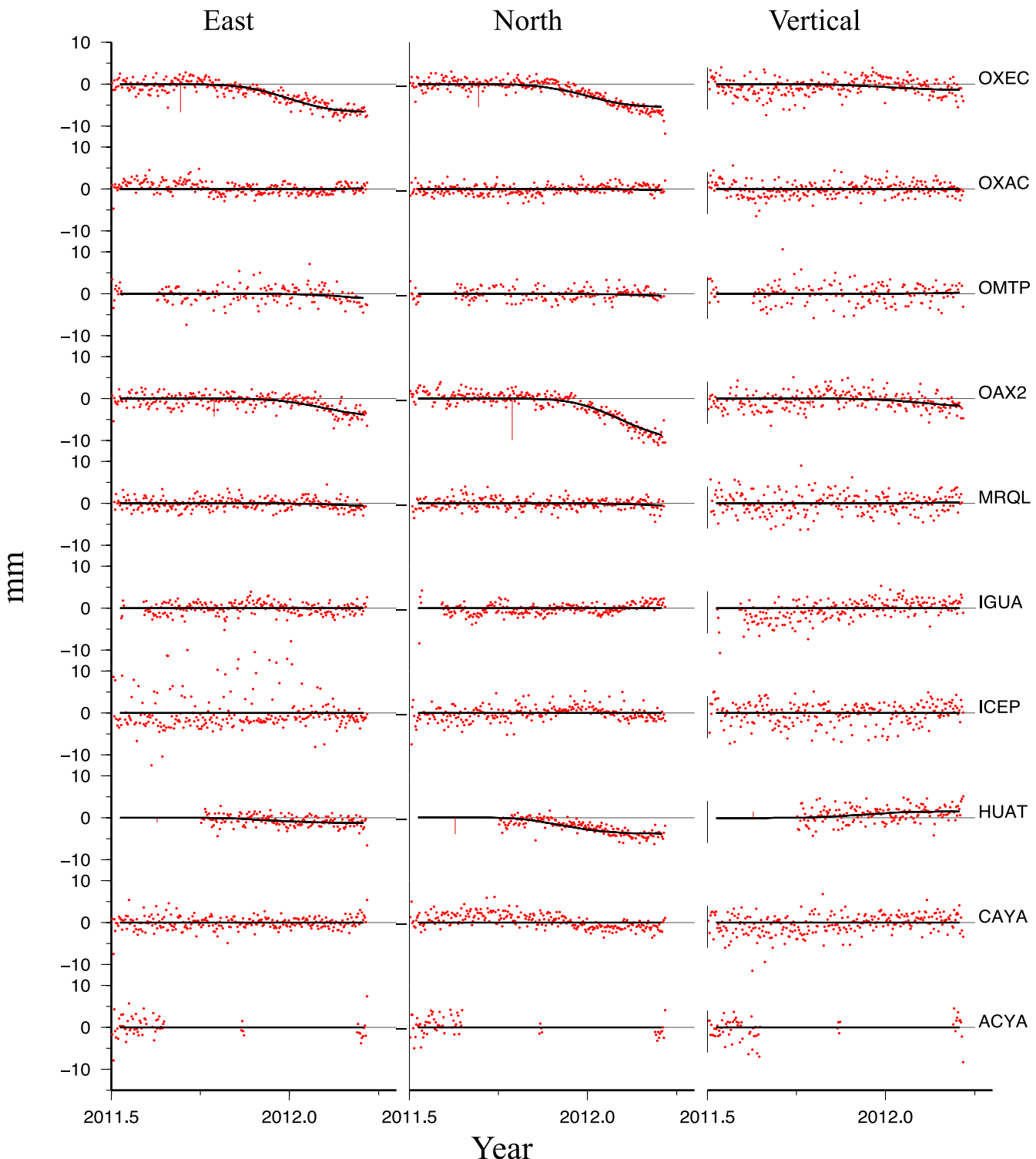
A1. Model fits to time series – All cGPS stations

Figure A1. Fits to GPS time series for the preferred SSE slip solution. Red circles show daily site positions reduced by the best-fitting slope prior to SSE onset

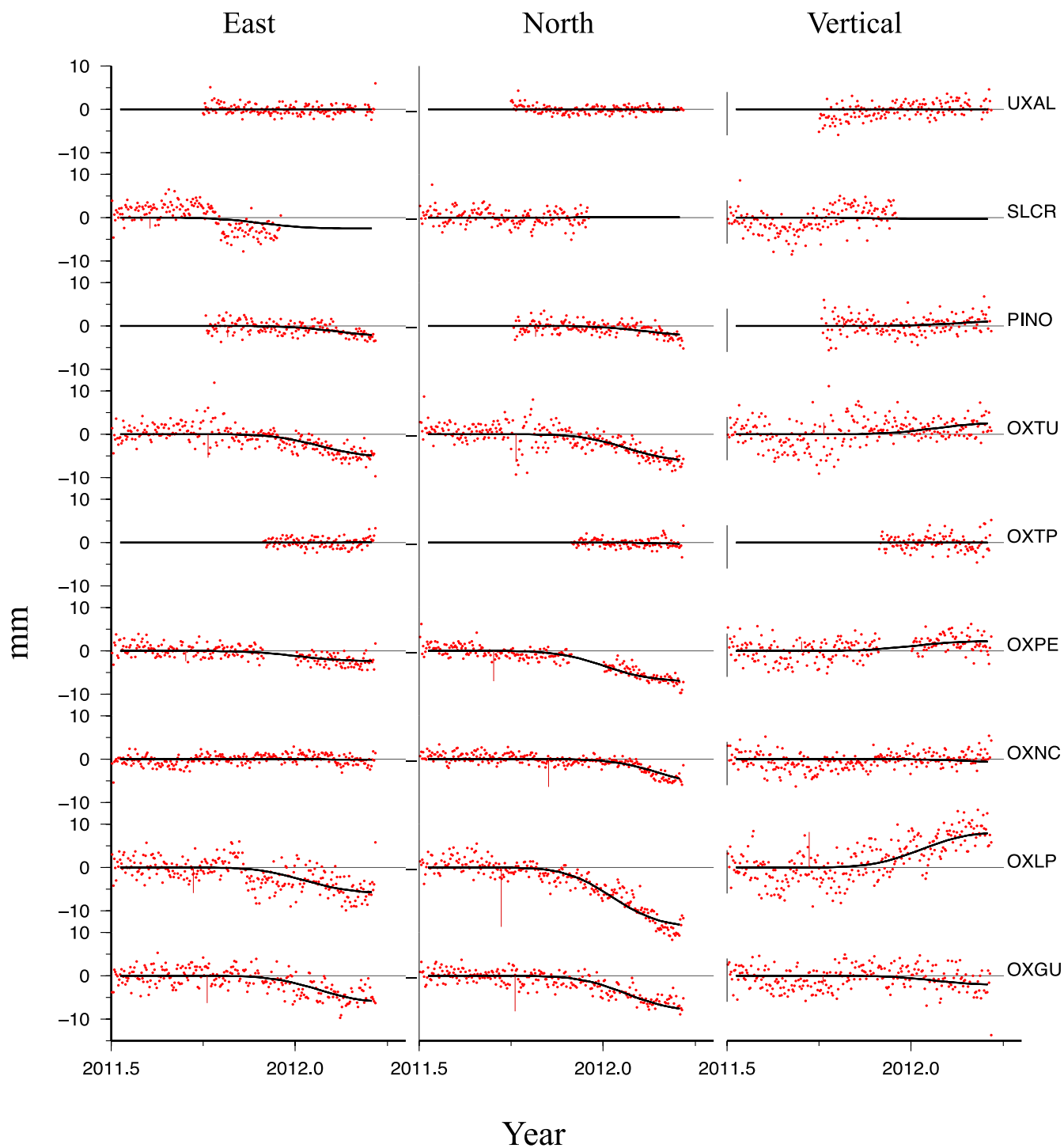


Figure A1. (Continued.)